

# Nano-topography sensing by osteoclasts

Dafna Geblinger<sup>1,2</sup>, Lia Addadi<sup>1</sup> and Benjamin Geiger<sup>2,\*</sup>

<sup>1</sup>Department of Structural Biology and <sup>2</sup>Department of Molecular Cell Biology, Weizmann Institute of Science, Rehovot 76100, Israel

\*Author for correspondence ([benny.geiger@weizmann.ac.il](mailto:benny.geiger@weizmann.ac.il))

Accepted 13 February 2010

*Journal of Cell Science* 123, 1503-1510

© 2010. Published by The Company of Biologists Ltd

doi:10.1242/jcs.060954

## Summary

Bone resorption by osteoclasts depends on the assembly of a specialized, actin-rich adhesive ‘sealing zone’ that delimits the area designed for degradation. In this study, we show that the level of roughness of the underlying adhesive surface has a profound effect on the formation and stability of the sealing zone and the associated F-actin. As our primary model substrate, we use ‘smooth’ and ‘rough’ calcite crystals with average topography values of 12 nm and 530 nm, respectively. We show that the smooth surfaces induce the formation of small and unstable actin rings with a typical lifespan of ~8 minutes, whereas the sealing zones formed on the rough calcite surfaces are considerably larger, and remain stable for more than 6 hours. It was further observed that steps or sub-micrometer cracks on the smooth surface stimulate local ring formation, raising the possibility that similar imperfections on bone surfaces may stimulate local osteoclast resorptive activity. The mechanisms whereby the physical properties of the substrate influence osteoclast behavior and their involvement in osteoclast function are discussed.

**Key words:** Osteoclast, Bone remodeling, Cytoskeleton, Biodegradable materials, Cell adhesion

## Introduction

Sensing of the chemical and physical features of the extracellular matrix (ECM) has a profound effect on the activity and fate of adherent cells. Variations in properties such as matrix molecular composition, adhesive ligand density, surface topography and compliance, can greatly affect many cellular processes, including adhesion, migration, ECM remodeling, cell proliferation, gene expression and cell viability (Bershadsky et al., 2006a; Chen et al., 1997; Diener et al., 2005; Discher et al., 2005; Engler et al., 2006; Geiger et al., 2009; Kunzler et al., 2007; Lo et al., 2000; Roach et al., 2007; Saltel et al., 2004; Vogel and Sheetz, 2006). In this work, we address the effects of adhesive surface nano-topography on the structure, dynamics and function of cultured osteoclasts.

Bone, composed of collagen fibers mineralized by carbonated apatite crystals (Weiner et al., 1999; Weiner and Wagner, 1998), is subject to continuous and tightly controlled remodeling, regulated primarily by two cell types, the bone-resorbing osteoclasts and the bone-depositing osteoblasts. Imbalance between their respective activities can lead to pathological conditions such as osteoporosis and osteopetrosis (Roodman, 1996).

Osteoclasts are giant multinucleated cells of the monocytic lineage (Blair, 1998). To degrade bone, osteoclasts adhere to the bone surface via specialized, actin-rich adhesion sites known as podosomes, which assemble into a ring-shaped ‘sealing zone’ (Luxenburg et al., 2007; Vaananen and Horton, 1995). The basic architecture of individual podosomes, and their general tendency to interact with each other via interconnecting actin fibers and form ring-like superstructures, is an intrinsic property of osteoclasts (Geblinger et al., 2009; Luxenburg et al., 2007). The sealing zone structure is composed of a central ring of actin filaments, flanked by inner and outer rings of integrins and several other adhesion proteins (Lakkakorpi and Vaananen, 1996; Mulari et al., 2003). The sealing zone mediates the tight attachment of the cell to the external surface, delimits the ‘resorption lacuna’ at the bone surface, and serves as a diffusion barrier that separates the resorption area from the rest of the extracellular space.

Bone degradation by osteoclasts is a complex process, regulated spatially and temporally at multiple levels, including the cytokine-mediated differentiation and homing of these cells, their adhesion to selected sites on the bone surface, and the assembly of the resorptive apparatus (Vaananen and Horton, 1995). It appears likely that osteoclasts sense, via their integrin-mediated adhesions, various features of the underlying matrix, including its chemical nature, level of mineralization, local rigidity, topography and the density of adhesive ligands. For example, the resorptive activity of osteoclasts on old bone is substantially higher than that on new bone (Henriksen et al., 2007); moreover, the assembly of a sealing zone occurs on selective and confined areas within the osteoclast-bone interface (Geblinger et al., 2009). Although indications for the adhesion-mediated surface sensing ability of osteoclasts are compelling, the nature of the specific bone features which are differentially sensed, and the cellular mechanisms triggered by them, are still unknown. Such information might be important not only for understanding the mechanisms governing the bone resorption process, but also for designing and fabricating novel resorbable implant materials that could serve as bone replacement, and eventually be remodeled into bone.

The specific surface feature investigated in this study is topography. Many cell types react to changes in the three-dimensional texture of the substrate at the nanometer- and micrometer scales, by altering their adhesion, motility and orientation (Cukierman et al., 2001; Curtis and Wilkinson, 1997; Geiger, 2001; Vogel and Sheetz, 2006). Fibroblasts and epithelial cells, for example, spread less and create smaller and fewer focal adhesions on rough metallic surfaces than on smooth ones (Baharloo et al., 2005; Grossner-Schreiber et al., 2006). Osteoblasts cultivated on metallic surfaces with nano- to micro-topography exhibit differences in their adhesion and spreading activity (Deligianni et al., 2001; Lange et al., 2002; Linez-Bataillon et al., 2002; Price et al., 2004). Thus, the spreading of osteoblasts was found to be stimulated at an ‘optimal’ roughness value, and reduced at higher or lower degrees of roughness (Huang et al., 2004).

Interestingly, the osteoblast response is affected not only by the roughness range, but also by the level of order in surface topography (Ball et al., 2008).

The effect of surface roughness on osteoclast activity has been far less characterized. Osteoclast resorptive activity on ceramic substrates was shown to be enhanced by introducing nanometer-scale roughness (Webster, 2001), and osteoclast differentiation was shown to be enhanced on rough metallic implant surfaces (Makihira et al., 2007; Marchisio et al., 2005). The mechanisms underlying the effect of surface roughness on the assembly of the osteoclast resorption apparatus have never been addressed.

In this study, we used calcite crystals ( $\text{CaCO}_3$ ) as our primary model substrate for osteoclasts, and examined the effect of surface nano-topography on sealing zone organization and dynamics. Calcite crystals express only one stable surface, the so-called 'cleavage rhombohedron' face, irrespective of surface roughness. The chemical properties of the rough and smooth surfaces are thus similar, enabling us to primarily address osteoclast response to surface roughness. We show herein that substrate roughness variations within a range of tens to hundreds of nanometers, induce major effects on sealing zone structure and dynamics. Osteoclasts cultured on smooth calcite surfaces form small and unstable rings, whereas rough surfaces induce the formation of large and stable peripheral sealing zones. We also show that small imperfections along the smooth surface (e.g. scratches and steps) locally stimulate ring formation, raising the possibility that bone surface features such as micro-cracks are sensed by osteoclasts, and activate the assembly of their resorption machinery.

## Results

Raw 264.7 osteoclasts were plated on large single crystals of calcite, a degradable mineral whose topography can be altered without changing the structure and composition of the surface. {104} is the crystallographic definition of the planes developed in the crystal as stable faces: it includes a family of six identical faces enclosing the crystal in different directions. The stable {104} cleavage surfaces of calcite are atomically smooth. Any attempt to cut calcite in other directions results in the formation of a rough surface composed of multiple {104} steps. In order to create a surface with distinct smooth and rough regions, single crystals of geological calcite were mechanically sawed halfway along planes intentionally different from {104}, enabling the remaining half to cleave spontaneously along {104}. The difference in surface topography was visualized by scanning electron microscopy (SEM) and measured by atomic force microscopy (AFM; Fig. 1). Representative areas of  $25 \times 25 \mu\text{m}$ , seven rough and ten smooth, from two different crystals were examined by AFM. The average roughness is defined as the average height of measured points relative to the mean plane. The measured average roughness ( $R_a$ ) values were  $530 \pm 290 \text{ nm}$  and  $12 \pm 6 \text{ nm}$  for the rough and smooth surfaces, respectively. Potential artifacts due to the AFM tip shape are negligible in this case, especially because the measurements are relative, and the sampling distribution is wide. The height histogram of the smooth surface is narrow, indicating a homogeneous surface, but the height histogram of the rough surface is rather wide, indicating the presence of a wide variety of altitudes (Fig. 1D,E).

In order to confirm the relevance of the roughness values in our model system to the nano-topography of natural bone, we employed SEM to examine untampered surfaces of murine humerus. The micrographs indicate that these natural bone surfaces exhibit a highly variable topography, ranging from smooth ( $R_a < 50 \text{ nm}$ ) to

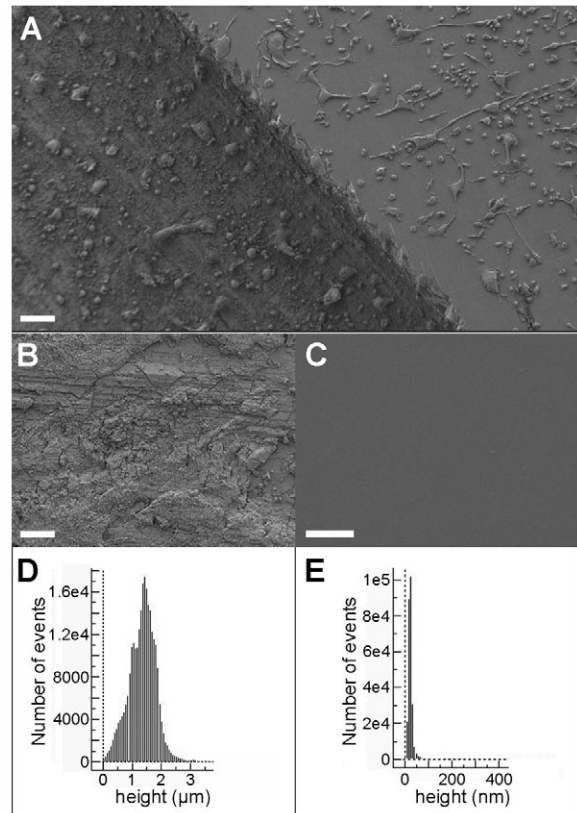


**Fig. 1. Smooth and rough calcite surfaces.** (A) Scanning electron micrograph of osteoclasts on a half-smooth, half-rough surface. Scale bar:  $100 \mu\text{m}$ . (B) Scanning electron micrograph of rough surface. Scale bar:  $20 \mu\text{m}$ . (C) Scanning electron micrograph of smooth surface. Scale bar:  $20 \mu\text{m}$ . (D) Histogram of height distribution on one representative  $25 \mu\text{m} \times 25 \mu\text{m}$  rough surface. (E) Histogram of height distribution on one representative  $25 \mu\text{m} \times 25 \mu\text{m}$  smooth surface.

rough ( $R_a \sim 1 \mu\text{m}$ ) surface landscapes (supplementary material Fig. S1). Hence, the range of calcite surface topographies examined is similar to those of genuine bone.

Osteoclasts stably expressing GFP-actin were cultured on the smooth and rough regions of the same crystal for 2–4 days, and continuously monitored by time-lapse fluorescence microscopy (1 image/minute) at multiple sites. Images were acquired, in parallel, from five cells adhering to the smooth region, and five adhering to the rough region of the same crystal. Osteoclasts adhering to the rough surfaces developed  $3 \pm 2$  large rings, delineating an area corresponding to  $43 \pm 17\%$  of the projected cell area ( $n=133$ ). Of these, 84% lasted for more than an hour (average  $>6$  hours;  $n=58$ ; Fig. 2, left panel; supplementary material Movie 1). By contrast, osteoclasts adhering to the smooth surfaces formed many small rings which, on average, dissolved within  $\sim 8$  minutes. None of these lasted for more than an hour ( $n=130$ ). The average number of rings coexisting in a cell was  $20 \pm 18$ ; nevertheless, they delineated an area corresponding to only  $4 \pm 2\%$  of the projected cell area ( $n=91$ ; Fig. 2, central panel; supplementary material Movie 2), and tended not to fuse with each other. Temporal ratio movies (see Materials and Methods) enabled visual comparison of the dynamic character of the rings formed on the two surfaces: a 'blue shift' in pixel color represents a decrease in actin intensity (in structures

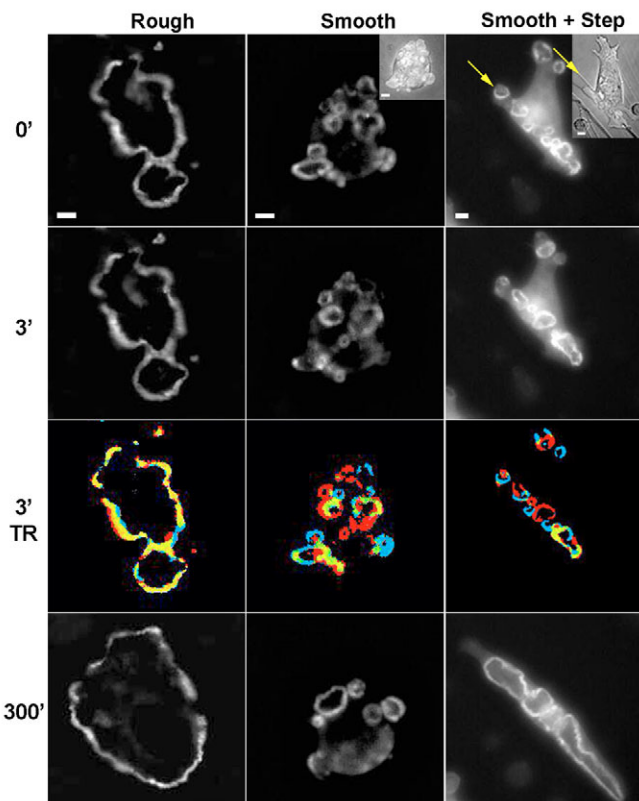


**Fig. 2. Frames from a time-lapse movie of the sealing zones on rough and smooth calcite surfaces, and on a step on the smooth surface, viewed at 0, 3 and 300 minutes.** The initial time point is arbitrary, approximately a day after replating. The temporal ratio (TR) between two time points, 3 minutes apart, is presented as a color code, such that new pixels are red, pixels that disappeared are blue, and unchanged pixels are yellow. Note the high proportion of red and blue pixels on the smooth surfaces, and the predominance of yellow pixels on the rough surface. Inserts depict transmitted light images of the cells on the surface at the beginning of the movie. Note the appearance of rings specifically along the step (arrows). Scale bars: 10  $\mu$ m.

undergoing dissociation), whereas a ‘red shift’ in pixel color indicates a local increase in intensity (in structures undergoing assembly). Actin ratio images in cells cultured on smooth surfaces are dominated by red and blue colors, indicating major rearrangements of actin within 3-minute periods. On rough surfaces, however, the dominant color was yellow, indicating pronounced structural stability (Fig. 2).

To examine the possible relationship between the loss of ring fusion and the high turnover of rings on the smooth surface, we measured the time needed for ring fusion to occur. Examination of 157 fusion events from 14 different cells, all plated on rough surfaces, indicated that the time interval between the formation of the first contacts between adjacent rings and actual ring fusion was  $8 \pm 4$  minutes. The fusion process consists of the apparent merger of neighboring actin rings, followed by a gap in the actin bundle around the middle of the overlap region. As this gap widens, the sealing zone grows (Fig. 3). Given that the lifespan of the small rings formed on the smooth surface is  $8 \pm 6$  minutes, and that only during part of that time (usually  $< 6$  minutes) adjacent rings are in visible contact with each other, it appears that the simplest

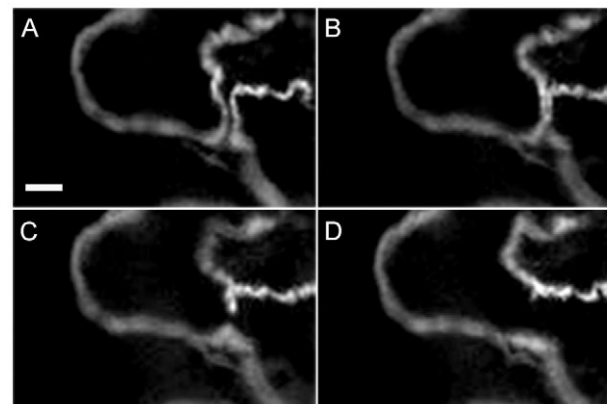


**Fig. 3. A fusion event.** (A) Sections of two individual rings, before touching. (B) The rings made contact, but had not yet fused. (C) Fusion of the rings. (D) After coalescence, a single ring is formed. Scale bar: 10  $\mu$ m.

explanation for the absence of ring fusion on the smooth surface is insufficient contact time.

Prolonged incubation of cells on the smooth surface led to the progressive formation of resorption pits, and thereby to local roughening of the surface underneath the cells (supplementary material Fig. S2). Consequently, over time, the cells on the initially smooth surface began to develop stable rings; after approximately 40–50 hours of incubation, the cells acquired a phenotype indistinguishable from that of cells cultured on rough surfaces (supplementary material Movie 3).

Visible steps present on the smooth surfaces of freshly-cleaved calcite crystals exerted a major effect on the formation of actin rings and eventually, on overall cell shape. This was manifested by the extensive nucleation of new, short-lived rings along the imperfection and, eventually, alignment of the entire cell body along it (Fig. 2, right panel; supplementary material Movie 4). The typical lifetime of these rings was similar to that of rings that formed on the smooth surface; moreover, these new rings tended not to fuse with each other. When incubated for longer periods of time (e.g. several hours), the rings formed around the imperfection tended to grow, become more stable, and fuse with each other, in conjunction with local roughening of the crystal surface by the attached cell (Fig. 2, right panel; supplementary material Movie 4). Three-minute temporal ratio imaging (supplementary material Movie 5), demonstrates the correlation between sealing zone size and stability, and changes induced in the surface topography. Specifically, the small, highly dynamic rings (mostly colored red and blue) were replaced, over time, by larger, more stable rings (colored yellow).

In principle, the differences in sealing zone organization and dynamics reported above could be attributed to either a direct cellular response to surface topography, or to higher local concentrations of adhesive proteins, mainly vitronectin. The latter mechanism could be expected, considering the fact that rough surfaces characterized by high surface energy usually show stronger protein adsorption (Kang and Lee, 2007; Rechendorff et al., 2006). To address this issue, the adsorption of vitronectin to the two surfaces was quantified by incubating them with various concentrations of vitronectin, to which traces of radio-iodinated vitronectin had been added. Following the incubation, the surfaces were rinsed, the radioactivity counted, and the amount of vitronectin

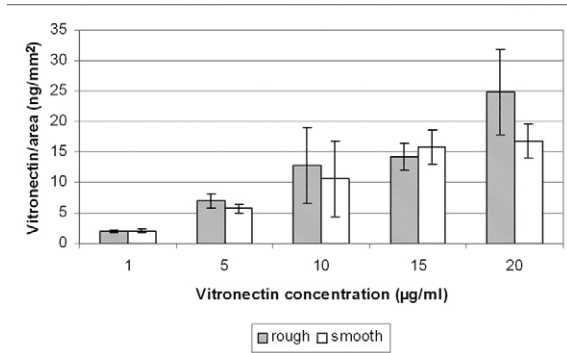


**Fig. 4. Vitronectin adsorption per unit area on rough and smooth calcite as a function of the concentration of vitronectin used for incubation.** Error bars represent standard deviations of measurements performed on four different crystals at each vitronectin concentration. At 10 µg/ml concentrations, vitronectin adsorption to smooth and rough calcite is similar; this is the concentration used in the experiments illustrated in Fig. 2. Note that a rough surface conditioned with 5 µg/ml vitronectin adsorbs much less than a smooth surface conditioned with 20 µg/ml vitronectin.

bound per unit area was calculated. Surprisingly, there was no significant difference in the amount of vitronectin bound to the smooth and rough calcite surfaces (Fig. 4). When the crystal surfaces were conditioned with a vitronectin concentration of 10 µg/ml, as used in previous experiments, the vitronectin densities on the rough and smooth surfaces were  $13 \pm 6$  ng/mm<sup>2</sup> and  $11 \pm 6$  ng/mm<sup>2</sup>, respectively. Furthermore, surface conditioning with different concentrations of vitronectin (resulting in smooth surfaces covered with  $17 \pm 3$  ng/mm<sup>2</sup> vitronectin, and rough surfaces covered with  $7 \pm 1$  ng/mm<sup>2</sup> vitronectin) had the same effect on sealing zone

properties as rough and smooth surfaces conditioned with identical vitronectin concentrations (Fig. 5).

To further reduce the likelihood that differential adsorption of other proteins, present in the medium or produced by the cells, is responsible for the differential osteoclast behavior, we passivated the calcite surface with an excess of BSA (1% overnight) after functionalizing it with 10 µg/ml vitronectin. Sealing zone formation in cells cultured on the smooth and on the rough surfaces remained dramatically different, irrespective of vitronectin concentration (supplementary material Fig. S3). These experiments demonstrate that surface topography, rather than the local concentration of vitronectin, is responsible for the differential behavior of osteoclasts on the rough and smooth substrates.

Is the differential response of osteoclasts to surface roughness a particular feature of calcite crystals, or a more general phenomenon? To address this issue, RAW osteoclasts were cultured on rough and smooth glass surfaces, and the organization and dynamics of their sealing zones were monitored. The surface roughness created on glass, measured by AFM, was similar to that formed on calcite,  $480 \pm 120$  nm and  $10 \pm 4$  nm on the rough and smooth glass, respectively. Examination of the sealing zone's overall morphology did not reveal significant differences in actin organization on the two surfaces. Thus, on both rough and smooth glass, similar, usually incomplete actin rings were formed, extending towards the cell periphery [for a detailed comparison of osteoclast behavior on glass, calcite and bone, see Geblinger et al. (Geblinger et al., 2009)]. However, the dynamic reorganization of the sealing zone was considerably slower on the rough glass (Fig. 6). Accordingly, on the smooth surface, the dominant colors in 1-minute temporal ratio images were red and blue, whereas on the rough surface, the dominant color was yellow. The correlation between frames, acquired 0–20 minutes apart, was calculated for time-lapse movies

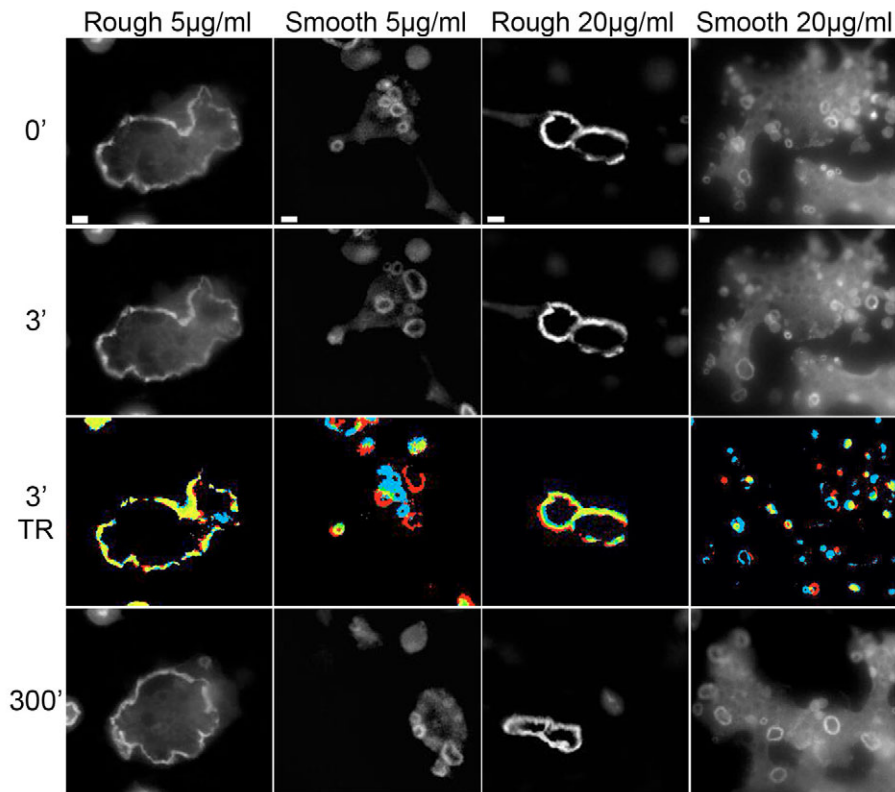


**Fig. 5. Frames from a time-lapse movie of the sealing zones of osteoclasts on rough and smooth calcite surfaces conditioned with 5 µg/ml and 20 µg/ml vitronectin, viewed at 0, 3 and 300 minutes.** The initial time point is arbitrary. Temporal ratio (TR) images are color-coded, as described for Fig. 2. Note that the dynamics, size and number of sealing zone rings depend on the topography of the calcite surface, regardless of the amount of vitronectin adsorbed. Scale bars: 10 µm.

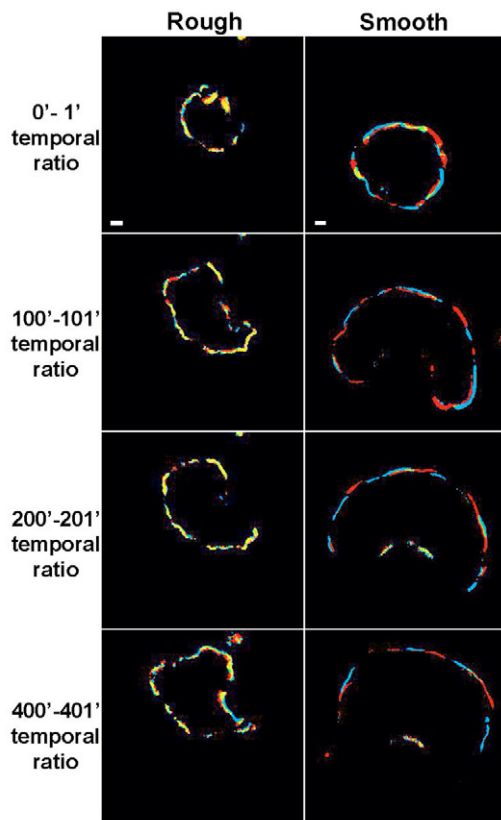


**Fig. 6. One-minute temporal ratio of osteoclast sealing zone rings on rough and smooth glass surfaces, viewed at 0, 100, 200 and 400 minutes.** The initial time point is arbitrary. The temporal ratio color code is as described in Fig. 2. Note the high proportion of red and blue pixels on the smooth surfaces, and the predominance of yellow pixels on the rough surface. Scale bars: 10  $\mu$ m.

of 15 cells on smooth glass, and 15 cells on rough glass (supplementary material Fig. S4). The initial decay in correlation was four times faster on the smooth surface, relative to the rough one. Moreover, the correlation between frames taken 10-20 minutes apart on the rough surface was approximately twice as high as that calculated for cells adhering to the smooth surface (supplementary material Fig. S4). We conclude that the topographical effect on sealing zone formation and dynamics is also present on glass, though sealing zone structure or size is not affected.

Thus far, the main criterion for assessing sealing zone dynamics has been the extent of reorganization of the actin cytoskeleton. One outstanding question is whether substrate micro-topography affects only the actin system, or whether it also alters the organization and turnover of the podosome adhesion machinery. To address this issue, we immunolabeled the GFP-actin-expressing cells for vinculin (a plaque protein, associated with the adhesive domain of the podosomes and sealing zone), and calculated the difference in net intensity of the two proteins in the sealing zone of osteoclasts cultured on the smooth and rough surfaces. The structure of the sealing zone observed on both the smooth and on the rough calcite consists of a ring of actin, flanked by inner and outer 'adhesive rings' containing plaque proteins such as vinculin and paxillin. The fluorescence intensity of actin in the sealing zone increased approximately fourfold in cells cultured on the rough

surface relative to the smooth surface, while the levels of vinculin did not significantly change (supplementary material Fig. S5). Moreover, the apparent instability of the sealing zone, monitored in osteoclasts co-expressing fluorescently-tagged derivatives of actin and paxillin, and cultured on smooth calcite, is similarly exhibited by the two proteins (data not shown). This implies that both the cytoskeletal and adhesive domains of the sealing zone share the same dynamic features induced by the topography of the surface.

## Discussion

Adhesion-mediated sensing of the local environment is a widespread cellular phenomenon, whereby cells collect information on the substrate on which they grow, integrate it, and develop a response (Bershadsky et al., 2006a; Chen et al., 1997; Diener et al., 2005; Discher et al., 2005; Engler et al., 2006; Geiger et al., 2009; Vogel and Sheetz, 2006). Among the diverse features that can be sensed by cells are surface chemistry (Leeuwenburgh et al., 2001; Monchau et al., 2002; Redey et al., 1999; Roach et al., 2007; Shimizu et al., 1989), local density of the adhesive ligands (Arnold et al., 2004; Arnold et al., 2008; Hirschfeld-Warneken et al., 2008), and physical properties (Bershadsky et al., 2006a; Bershadsky et al., 2006b; Engler et al., 2006; Vogel and Sheetz, 2006). In the present study, we specifically addressed the ability of one particular cell type to sense surface topography; namely, the osteoclast, the primary function of which is to remodel the underlying surface.

We recently demonstrated that multiple aspects of actin organization, structure and dynamics in osteoclasts are affected by the nature of the surface, and that on bone, some areas are more prone than others to locally-induced formation of the adhesive apparatus (Geblinger et al., 2009). Thus, beneath the same cell, certain regions of the substrate are constantly visited by sealing zone rings, while others remain untouched. This indicates that the area to be degraded is not only determined by the initial 'decision' of the cell to adhere to a particular site, but that, within this site, specific areas are targeted for resorption. Bone properties change with time, as a result of continuous changes in mineralization, and accumulation of damage. Moreover, the resorption process itself results in major alterations in bone surface properties and, hence, further affects the resorptive activities of the cell. It is thus conceivable that the surface properties are partially, if not fully, responsible for generating signals that, in turn, control cell behavior.

In order to determine which surface features affect osteoclast response, well-characterized surfaces must be used as adhesive substrates. Large single calcite crystals serve as a useful model, because the unique, stable surface guarantees that the same chemistry is exposed on the surface, regardless of the topography induced. Experiments conducted simultaneously on smooth and rough areas of the same single crystal ensure that environmental conditions such as temperature and medium, or even impurities in the crystal itself, do not affect the results. Furthermore, examination of cell behavior on calcite surfaces functionalized with different densities of adhesion proteins, indicates that differential adsorption of proteins cannot account for the observed differences in adhesion dynamics. We thus conclude that the major parameter differentially influencing cell behavior on the rough and smooth calcite surfaces is surface topography.

We demonstrate that topography, per se, influences the dynamic organization of the osteoclast resorption apparatus. We further show that whereas the rough surface induces the formation of large and stable sealing zone rings, on the smooth surface only small and

unstable rings are formed. The average lifespan of rings formed on the smooth surface is of the same order as the minimal contact time needed for sealing zone fusion; hence, the rings formed on the smooth surfaces fail to fuse, most likely because of insufficient contact time. Direct testing of this hypothesis is currently underway.

Surface nano-topography appears to regulate not only the dynamics of the 'resorptive ring', but also its initiation. Thus, visible steps and imperfections along the otherwise smooth crystal surface provide signals for initiation of ring formation in specific locations underneath the cell, and eventually lead to cell body orientation. Notably, the adherent osteoclasts do not just respond to the topography of the surface, but also actively modify it. Thus, when cells are incubated for prolonged periods on a smooth calcite surface, they locally 'roughen' the underlying surface which, in turn, induces the formation of large and considerably more stable sealing zones.

Experiments in which cell behavior on rough and smooth glass surfaces was compared, indicate that some, but not all, features of the cellular response to rough calcite also apply to glass. Thus, roughness on glass surfaces increases ring stability and reduces its turnover rate, similar to roughness on calcite, whereas it does not affect the absence of ring coherence that is a fundamental characteristic of osteoclast behavior on glass (Geblinger et al., 2009). It is clear that certain parameters affect cell and ring dynamics per se, while other parameters are responsible for ring integrity, as well as the inception and fate of the resorption activity. The multiplicity of parameters affecting cell behavior is, in itself, not surprising. The difficulty lies in unraveling the contribution of each, and the cross-talk between them.

Particularly challenging is the relevance of the data described herein to the situation *in vivo*. The range of topographies examined here using artificial surfaces is similar to those present on genuine bone, and is therefore physiologically relevant. Moreover, it is conceivable that old and damaged bone is considerably rougher than newly-formed bone, because in the former, crystals growing within the collagen fibrils emerge from the collagen gap zone channels, changing both the chemistry and the physical properties of the bone surface.

What is the mechanism underlying the cell's ability to sense, and respond to, nano-topography? Studies in recent years have established that integrin-mediated matrix adhesions act as 'environmental sensors', whereby cells can identify and respond to chemical and physical properties of the underlying matrix, such as rigidity, mechanical activity, ligand density and dimensionality (Bershadsky et al., 2006a; Chen et al., 1997; Diener et al., 2005; Discher et al., 2005; Engler et al., 2006; Geiger et al., 2009; Vogel and Sheetz, 2006). Cell sensing of the environment plays a key role in integrin immobilization and activation, leading to formation of an adhesion complex. Furthermore, the development of adhesion sites, including activation of signaling activity at the cell interior and interaction with the cytoskeleton, are all strongly affected by the physical nature of the matrix.

Several mechanisms underlying the cellular response to topographical features have been suggested for a variety of cell types (Balaban et al., 2001; Gov and Gopinathan, 2006; Patel et al., 2001; Riveline et al., 2001; Tarricone et al., 2001; Ulmer et al., 2008; Van Aelst et al., 1996; Vogel and Sheetz, 2006). Surface roughness may induce the ventral cell membrane to adapt to a rough topography, leading to an uneven distribution of proteins (e.g. bar-domain proteins) that tend to partition into areas of high curvature (Gov and Gopinathan, 2006; Tarricone et al., 2001; Van

Aelst et al., 1996; Vogel and Sheetz, 2006). Other targets that could be affected by topography are ion channels, which open and close as a result of structural changes induced by the local geometry of the membrane. Such channels could affect signaling activity at the adhesion sites (Patel et al., 2001; Vogel and Sheetz, 2006). Another possibility is that the topography of the surface induces conformational changes in proteins such as fibronectin that are adsorbed on the surface, thus exposing specific binding sites within the protein that are hidden when the protein is adsorbed on a flat surface (Ulmer et al., 2008). Surface nano-topography may also greatly affect the mechanical forces locally applied by the attached cytoskeleton to the membrane at the adhesion sites. Mechanical force applied to integrin adhesions was shown to strongly influence adhesion formation and dynamics (Balaban et al., 2001; Riveline et al., 2001). The interplay between topography, force and adhesion dynamics might also affect other, mechanosensitive adhesions such as focal adhesions, possibly accounting for changes in their stability, signaling activity and dynamics, when plated on a rough three-dimensional matrix (Cukierman et al., 2001). Whether focal adhesions and podosomes are regulated by surface micro-topography in a similar manner, remains to be determined. Although the mechanisms underlying these sensory functions are poorly understood, growing evidence suggests that protein unfolding, and reorganization of multiprotein complexes, play a key role in this process (Geiger et al., 2009; Wolfenson et al., 2009).

How is surface topography sensed? We have previously shown that actin-containing sealing zones formed on various surfaces (e.g. glass, calcite and bone) differ in their thickness, podosome-to-podosome distance, and density of actin fibers interconnecting the constituting podosomes (Geblinger et al., 2009). Here, we show that the fluorescence intensity of actin in the sealing zone is approximately fourfold higher on the rough surface than on the smooth surface, while the levels of vinculin do not differ significantly. This observation strongly supports the notion that the density of actin in the sealing zone structure is closely correlated to its stability; namely, that more stable rings enable the development of larger, denser and more interconnected podosomes. Attempts to identify the cellular components (e.g. cortactin) that upregulate actin polymerization on the rough surfaces, and their mode of activation, are currently underway. The fact that vinculin intensity is essentially the same on both types of surface implies that the local concentration of this plaque protein does not directly regulate the dynamics of the sealing zone.

The possibility that microtubules may play a role in the regulation of osteoclast behavior on rough surfaces was also considered (Evans et al., 2003). Interestingly, when nocodazole, which destroys microtubules, was added to osteoclasts adhering to rough surfaces, it induced the formation of smaller, more dynamic rings (supplementary material Movie 6), in line with the findings of Destaing et al. (Destaing et al., 2003). However, the mechanisms whereby surface roughness affects microtubules, and the nature of the microtubule-induced effect on the actin-integrin system, require further investigation.

When attempting to analyze the mechanisms whereby topography may control osteoclast activity, it must be kept in mind that sealing zone rings encompass areas ranging from micrometers to tens of micrometers in diameter. The individual 'adhesion units' forming the ring, the podosomes, are typically 0.5-1  $\mu\text{m}$  across, and are interconnected by a dense network of fibers. The podosomal unit itself consists of a core actin bundle, connected to an integrin-containing adhesion ring via radial fibers. The architecture of the

podosomes, and the manner in which they assemble into sealing zones, are similar on calcite, bone and glass (Geblinger et al., 2009; Luxenburg et al., 2007). The entire ring behaves as a single, complex network built of core units communicating with each other via the cytoskeleton, as well as with the substrate, through the podosomal adhesion plaque (Luxenburg et al., 2007). The assembly of this unique architecture, together with the evidence that actomyosin-based contractility affects podosome turnover (van Helden et al., 2008), suggest that mechanical forces generated by the sealing zone may regulate podosome assembly, and hence, sealing zone turnover. Notably, although podosomal adhesions share with integrin-mediated focal adhesions the ability to respond to different features of the adhesive surface, the dimensions and cytoskeletal organization of the two adhesions differ greatly.

Substrate adhesion is regulated in osteoclasts at different orders of magnitude. Thus, the interaction of integrin with the extracellular matrix occurs on a scale of 0.1  $\mu\text{m}$ ; integrin adhesions communicate directly with podosomes, which span an area of  $\sim 1 \mu\text{m}^2$ ; whereas sealing zones, resulting from the assembly of many podosomes, have radii on the order of 10  $\mu\text{m}$ . Thus, initial interactions resulting from molecular forces are translated, through three orders of magnitude, into local (podosomal) forces and, finally, into a global, sealing zone response.

It is conceivable that topography within the 0.1–1  $\mu\text{m}$  range, which characterizes the rough surfaces studied here, may be sensed through forces applied at varying heights and angles of the surface to the expanding ring, through the radial fibers and the interconnected cores.

Thus, while a smooth surface would be expected to induce steady-state equilibrium in the relative distribution of lengths and, consequently, forces applied to the radial fibers and sensed by cores, a rough surface, with its perpetually changing terrain, would translate into a heterogeneous landscape of forces that could be read by the cell as a stimulus for stability. At this stage, these are stimulating hypotheses that need to be challenged experimentally.

Clearly, no single surface parameter can be expected to control overall osteoclast behavior. Therefore, each parameter must be analyzed in depth, before its effect can be considered alongside that of other physical or chemical features affecting osteoclast behavior. Our ultimate aim is to integrate all of the information collected on isolated parameters, and provide a comprehensive view of the mechanisms by which osteoclasts sense substrate features. This goal is by no means easily met but, once achieved, should improve our understanding of bone remodeling processes.

## Materials and Methods

### Tissue culture and substrate preparation

RAW 264.7 cells obtained from the American Type Culture Collection (ATCC; Manassas, VA, USA), were cultured at 37°C in a 5% CO<sub>2</sub> humidified atmosphere in DMEM with Earle's salts, L-glutamine and NaHCO<sub>3</sub>, supplemented with fetal bovine serum and antibiotics. To induce osteoclast differentiation, cells were plated at a density of 100 cells/mm<sup>2</sup> in alpha-MEM medium supplemented with soluble receptor activator of NF- $\kappa$ B ligand (RANK-L; 20 ng/ml), and macrophage colony-stimulating factor (M-CSF; 20 ng/ml). After 3 days, cells were removed with EDTA (10 mM) for 10 minutes, and then plated for 60 hours on thin slices of calcite with surfaces of variable roughness.

Calcite single crystal slices, 5–10 mm wide and 0.5–1 mm thick, were partly mechanically sawn from a geological crystal at an angle that differed from the stable cleavage plane, thus creating a surface with multiple steps, then cleaved. The glass surfaces were created by taking a glass slide and polishing it with a polish paper (400 grit) using a polishing instrument for reproducibility. Surfaces were immersed in 70% ethanol for 10 minutes, and conditioned with vitronectin (10  $\mu\text{g}/\text{ml}$ ) for 8–10 hours at 4°C. Prior to cell plating, the calcite slices were washed, placed in the culture medium, and heated to 37°C.

### Fluorescence microscopy

For live cell imaging, RAW cells stably expressing GFP-actin (Luxenburg et al., 2006) were induced to differentiate in plastic dishes for 3 days, then suspended and replated on calcite slices as described above, and observed for 60 hours in sequential periods of 8–12 hours, starting 4 hours after replating, using a DeltaVision microscopy system (Applied Precision, Inc.) consisting of an IX70 inverted microscope equipped with a  $\times 20/0.7$  NA objective (Olympus).

Image processing and analysis was carried out using Priism software for Linux operating systems (<http://msg.ucsf.edu/IVE/Download/>). Temporal ratio images were produced as previously described (Zamir et al., 1999). Briefly, the pixel intensity values of frame  $t+x$  were divided by the intensity values of the corresponding pixel at time  $t$ , producing a 'spectral image' in which blue pixels indicate new structures, and red pixels indicate faded structures. Intermediate colors represent variations in local fluorescence intensity.

### Radioactive labeling

Vitronectin (16  $\mu\text{g}$ , 50  $\mu\text{g}/\text{ml}$ ) was iodinated, using chloramine-T (10  $\mu\text{l}$ , 1 mg/ml). <sup>125</sup>I (5  $\mu\text{l}$ , 0.5 mCi) was added, mixed, and after 2 minutes at room temperature, sodium metabisulfate (10  $\mu\text{l}$ , 1 mg/ml) was added for 2 minutes. KI (50  $\mu\text{l}$ , 50 mg/ml) was then added, and the solution was chromatographed on a column of Sephadex G-25 medium, while being monitored with a Geiger counter. The first radioactive peak (1.2 ml), containing the radiolabeled vitronectin, was then collected.

To measure the amount of vitronectin associated with the rough and smooth crystal surfaces, unlabeled vitronectin was mixed with traces of the iodinated protein and 30  $\mu\text{l}$  aliquots containing 1, 5, 10, 15 or 20  $\mu\text{g}/\text{ml}$  of vitronectin were applied to the two surfaces. Crystals were incubated for 16 hours at 4°C, then washed three times in PBS for 5 minutes each, and placed in a test tube in 1 ml PBS. Radioactivity was then measured using a gamma counter (Cobra II Auto-Gamma, Packard).

### Mouse bone preparation

The humerus bone was extracted from C57BL/6 postnatal day 2 mice. The bone was transversely freeze-fractured and cleaned in 1% sodium hypochloride for 2 minutes, washed with water, and dehydrated with ethanol. The samples were finally air-dried, and coated with chromium.

### Measurement of actin and vinculin

GFP-actin expressing cells were cultured on smooth and rough surfaces for 24 hours prior to permeabilization with 0.5% Triton X-100, and fixation with 3% PFA. Cells were immunolabeled with mouse anti-vinculin (clone hVIN-1; Sigma) and then stained with goat anti-mouse secondary antibody conjugated to cy-5 (Jackson ImmunoResearch). The images were used for analysis were taken using a DeltaVision microscopy system (Applied Precision, Inc.) consisting of an IX70 inverted microscope equipped with a 40 $\times$  objective (Olympus).

We thank Bilha Schechter for her help with the radioactive labeling and measurements, Roy Ziblat for his assistance with the AFM measurements, Zvi Kam for guidance in image processing, Amnon Sharir for providing us with mouse bone, Julia Mahamid for assisting with bone sample preparations for SEM, and Barbara Morgenstern for editorial assistance. This study was supported by a grant from the Israel Science Foundation, and an NIGMS grant to the Cell Migration Consortium (NIH grant U54GM64346). Electron microscopy studies were conducted at the Irving and Cherna Moskowitz Center for Nano and Bio-Nano Imaging at the Weizmann Institute of Science. B.G. holds the Erwin Neter Professorial Chair in Cell and Tumor Biology. L.A. holds the Dorothy and Patrick E. Gorman Professorial Chair of Biological Ultrastructure. Deposited in PMC for release after 12 months.

Supplementary material available online at

<http://jcs.biologists.org/cgi/content/full/123/9/1503/DC1>

## References

- Arnold, M., Cavalcanti-Adam, E. A., Glass, R., Blummel, J., Eck, W., Kantschler, M., Kessler, H. and Spatz, J. P. (2004). Activation of integrin function by nanopatterned adhesive interfaces. *Chemphyschem* **5**, 383–388.
- Arnold, M., Hirschfeld-Warneken, V. C., Lohmuller, T., Heil, P., Blummel, J., Cavalcanti-Adam, E. A., Lopez-Garcia, M., Walther, P., Kessler, H., Geiger, B. et al. (2008). Induction of cell polarization and migration by a gradient of nanoscale variations in adhesive ligand spacing. *Nano. Lett.* **8**, 2063–2069.
- Baharloo, B., Textor, M. and Brunette, D. M. (2005). Substratum roughness alters the growth, area, and focal adhesions of epithelial cells, and their proximity to titanium surfaces. *J. Biomed. Mater. Res. A* **74**, 12–22.
- Balaban, N. Q., Schwarz, U. S., Riveline, D., Goichberg, P., Tzur, G., Sabanay, I., Mahalu, D., Safran, S., Bershadsky, A., Addadi, L. et al. (2001). Force and focal adhesion assembly: a close relationship studied using elastic micropatterned substrates. *Nat. Cell Biol.* **3**, 466–472.

- Ball, M., Grant, D. M., Lo, W. J. and Scotchford, C. A. (2008). The effect of different surface morphology and roughness on osteoblast-like cells. *J. Biomed. Mater. Res. A* **86**, 637-647.
- Bershadsky, A., Kozlov, M. and Geiger, B. (2006a). Adhesion-mediated mechanosensitivity: a time to experiment, and a time to theorize. *Curr. Opin. Cell Biol.* **18**, 472-481.
- Bershadsky, A. D., Ballestrem, C., Carramusa, L., Zilberman, Y., Gilquin, B., Khochbin, S., Alexandrova, A. Y., Verkhovsky, A. B., Shemesh, T. and Kozlov, M. M. (2006b). Assembly and mechanosensory function of focal adhesions: experiments and models. *Eur. J. Cell Biol.* **85**, 165-173.
- Blair, H. C. (1998). How the osteoclast degrades bone. *BioEssays* **20**, 837-846.
- Chen, C. S., Mrksich, M., Huang, S., Whitesides, G. M. and Ingber, D. E. (1997). Geometric control of cell life and death. *Science* **276**, 1425-1428.
- Cukierman, E., Pankov, R., Stevens, D. R. and Yamada, K. M. (2001). Taking cell-matrix adhesions to the third dimension. *Science* **294**, 1708-1712.
- Curtis, A. and Wilkinson, C. (1997). Topographical control of cells. *Biomaterials* **18**, 1573-1583.
- Deligianni, D. D., Katsala, N. D., Koutsoukos, P. G. and Missirlis, Y. F. (2001). Effect of surface roughness of hydroxyapatite on human bone marrow cell adhesion, proliferation, differentiation and detachment strength. *Biomaterials* **22**, 87-96.
- Destaing, O., Saltel, F., Geminard, J. C., Jurdic, P. and Bard, F. (2003). Podosomes display actin turnover and dynamic self-organization in osteoclasts expressing actin-green fluorescent protein. *Mol. Biol. Cell* **14**, 407-416.
- Diener, A., Nebe, B., Luthen, F., Becker, P., Beck, U., Neumann, H. G. and Rychly, J. (2005). Control of focal adhesion dynamics by material surface characteristics. *Biomaterials* **26**, 383-392.
- Discher, D. E., Janmey, P. and Wang, Y. L. (2005). Tissue cells feel and respond to the stiffness of their substrate. *Science* **310**, 1139-1143.
- Engler, A. J., Sen, S., Sweeney, H. L. and Discher, D. E. (2006). Matrix elasticity directs stem cell lineage specification. *Cell* **126**, 677-689.
- Evans, J. G., Correia, I., Krasavina, O., Watson, N. and Matsudaira, P. (2003). Macrophage podosomes assemble at the leading lamella by growth and fragmentation. *J. Cell Biol.* **161**, 697-705.
- Geblinger, D., Geiger, B. and Addadi, L. (2009). Surface-induced regulation of podosome organization and dynamics in cultured osteoclasts. *Chembiochem* **10**, 158-165.
- Geiger, B. (2001). Cell biology. Encounters in space. *Science* **294**, 1661-1663.
- Geiger, B., Spatz, J. P. and Bershadsky, A. D. (2009). Environmental sensing through focal adhesions. *Nat. Rev. Mol. Cell Biol.* **10**, 21-33.
- Gov, N. S. and Gopinathan, A. (2006). Dynamics of membranes driven by actin polymerization. *Biophys. J.* **90**, 454-469.
- Grossner-Schreiber, B., Herzog, M., Hedderich, J., Duck, A., Hannig, M. and Griepentrog, M. (2006). Focal adhesion contact formation by fibroblasts cultured on surface-modified dental implants: an in vitro study. *Clin. Oral Implants Res.* **17**, 736-745.
- Henriksen, K., Leeming, D. J., Byrjalsen, I., Nielsen, R. H., Sorensen, M. G., Dziegiel, M. H., Martin, T. J., Christiansen, C., Qvist, P. and Karsdal, M. A. (2007). Osteoclasts prefer aged bone. *Osteoporos. Int.* **18**, 751-759.
- Hirschfeld-Warneken, V. C., Arnold, M., Cavalcanti-Adam, A., Lopez-Garcia, M., Kessler, H. and Spatz, J. P. (2008). Cell adhesion and polarisation on molecularly defined spacing gradient surfaces of cyclic RGDfK peptide patches. *Eur. J. Cell Biol.* **87**, 743-750.
- Huang, H. H., Ho, C. T., Lee, T. H., Lee, T. L., Liao, K. K. and Chen, F. L. (2004). Effect of surface roughness of ground titanium on initial cell adhesion. *Biomol. Eng.* **21**, 93-97.
- Kang, C. K. and Lee, Y. S. (2007). The surface modification of stainless steel and the correlation between the surface properties and protein adsorption. *J. Mater. Sci. Mater. Med.* **18**, 1389-1398.
- Kunzler, T. P., Drobek, T., Schuler, M. and Spencer, N. D. (2007). Systematic study of osteoblast and fibroblast response to roughness by means of surface-morphology gradients. *Biomaterials* **28**, 2175-2182.
- Lakkakorpi, P. T. and Vaananen, H. K. (1996). Cytoskeletal changes in osteoclasts during the resorption cycle. *Microsc. Res. Tech.* **33**, 171-181.
- Lange, R., Luthen, F., Beck, U., Rychly, J., Baumann, A. and Nebe, B. (2002). Cell-extracellular matrix interaction and physico-chemical characteristics of titanium surfaces depend on the roughness of the material. *Biomol. Eng.* **19**, 255-261.
- Leeuwenburgh, S., Layrolle, P., Barrere, F., de Bruijn, J., Schoonman, J., van Blitterswijk, C. A. and de Groot, K. (2001). Osteoclastic resorption of biomimetic calcium phosphate coatings in vitro. *J. Biomed. Mater. Res.* **56**, 208-215.
- Linez-Bataillon, P., Monchau, F., Bigerelle, M. and Hildebrand, H. F. (2002). In vitro MC3T3 osteoblast adhesion with respect to surface roughness of Ti6Al4V substrates. *Biomol. Eng.* **19**, 133-141.
- Lo, C. M., Wang, H. B., Dembo, M. and Wang, Y. L. (2000). Cell movement is guided by the rigidity of the substrate. *Biophys. J.* **79**, 144-152.
- Luxenburg, C., Parsons, J. T., Addadi, L. and Geiger, B. (2006). Involvement of the Src-cortactin pathway in podosome formation and turnover during polarization of cultured osteoclasts. *J. Cell Sci.* **119**, 4878-4888.
- Luxenburg, C., Geblinger, D., Klein, E., Anderson, K., Hanein, D., Geiger, B. and Addadi, L. (2007). The architecture of the adhesive apparatus of cultured osteoclasts: from podosome formation to sealing zone assembly. *PLoS ONE* **2**, e179.
- Makihira, S., Mine, Y., Kosaka, E. and Nikawa, H. (2007). Titanium surface roughness accelerates RANKL-dependent differentiation in the osteoclast precursor cell line, RAW264.7. *Dent. Mater. J.* **26**, 739-745.
- Marchisio, M., Di Carmine, M., Pagone, R., Piattelli, A. and Miscia, S. (2005). Implant surface roughness influences osteoclast proliferation and differentiation. *J. Biomed. Mater. Res. B Appl. Biomater.* **75**, 251-256.
- Monchau, F., Lefevre, A., Descamps, M., Belquin-myrdycz, A., Laffargue, P. and Hildebrand, H. F. (2002). In vitro studies of human and rat osteoclast activity on hydroxyapatite, beta-tricalcium phosphate, calcium carbonate. *Biomol. Eng.* **19**, 143-152.
- Mulari, M., Vaaranen, J. and Vaananen, H. K. (2003). Intracellular membrane trafficking in bone resorbing osteoclasts. *Microsc. Res. Tech.* **61**, 496-503.
- Patel, A. J., Lazdunski, M. and Honore, E. (2001). Lipid and mechano-gated 2P domain K(+) channels. *Curr. Opin. Cell Biol.* **13**, 422-428.
- Price, R. L., Ellison, K., Haberstroh, K. M. and Webster, T. J. (2004). Nanometer surface roughness increases select osteoblast adhesion on carbon nanofiber compacts. *J. Biomed. Mater. Res. A* **70**, 129-138.
- Rechenhorff, K., Hovgaard, M. B., Foss, M., Zhdanov, V. P. and Besenbacher, F. (2006). Enhancement of protein adsorption induced by surface roughness. *Langmuir* **22**, 10885-10888.
- Redey, S. A., Razzouk, S., Rey, C., Bernache-Assollant, D., Leroy, G., Nardin, M. and Cournot, G. (1999). Osteoclast adhesion and activity on synthetic hydroxyapatite, carbonated hydroxyapatite, and natural calcium carbonate: relationship to surface energies. *J. Biomed. Mater. Res.* **45**, 140-147.
- Riveline, D., Zamir, E., Balaban, N. Q., Schwarz, U. S., Ishizaki, T., Narumiya, S., Kam, Z., Geiger, B. and Bershadsky, A. D. (2001). Focal contacts as mechanosensors: externally applied local mechanical force induces growth of focal contacts by an mDia1-dependent and ROCK-independent mechanism. *J. Cell Biol.* **153**, 1175-1186.
- Roach, P., Eglin, D., Rohde, K. and Perry, C. C. (2007). Modern biomaterials: a review-bulk properties and implications of surface modifications. *J. Mater. Sci. Mater. Med.* **18**, 1263-1277.
- Roodman, G. D. (1996). Advances in bone biology: the osteoclast. *Endocr. Rev.* **17**, 308-332.
- Saltel, F., Destaing, O., Bard, F., Eichert, D. and Jurdic, P. (2004). Apatite-mediated actin dynamics in resorbing osteoclasts. *Mol. Biol. Cell* **15**, 5231-5241.
- Shimizu, H., Sakamoto, S., Sakamoto, M. and Lee, D. D. (1989). The effect of substrate composition and condition on resorption by isolated osteoclasts. *Bone Miner.* **6**, 261-275.
- Tarricone, C., Xiao, B., Justin, N., Walker, P. A., Rittinger, K., Gamblin, S. J. and Smerdon, S. J. (2001). The structural basis of Arp2/3-mediated cross-talk between Rac and Arp signalling pathways. *Nature* **411**, 215-219.
- Ulmer, J., Geiger, B. and Spatz, J. P. (2008). Force-induced fibronectin fibrillogenesis in vitro. *Soft Matter* **4**, 1998-2007.
- Vaananen, H. K. and Horton, M. (1995). The osteoclast clear zone is a specialized cell-extracellular matrix adhesion structure. *J. Cell Sci.* **108**, 2729-2732.
- Van Aelst, L., Joneson, T. and Bar-Sagi, D. (1996). Identification of a novel Rac1-interacting protein involved in membrane ruffling. *EMBO J.* **15**, 3778-3786.
- van Helden, S. F., Oud, M. M., Joosten, B., Peterse, N., Figdor, C. G. and van Leeuwen, F. N. (2008). PGE2-mediated podosome loss in dendritic cells is dependent on actomyosin contraction downstream of the RhoA-Rho-kinase axis. *J. Cell Sci.* **121**, 1096-1106.
- Vogel, V. and Sheetz, M. (2006). Local force and geometry sensing regulate cell functions. *Nat. Rev. Mol. Cell Biol.* **7**, 265-275.
- Webster, T. J. (2001). Nanoceramic surface roughness enhances osteoblast and osteoclast functions for improved orthopaedic/dental implant efficacy. *Scr. Mater.* **44**, 1639-1642.
- Weiner, S. and Wagner, H. D. (1998). The material bone: Structure mechanical function relations. *Annu. Rev. Mat. Sci.* **28**, 271-298.
- Weiner, S., Traub, W. and Wagner, H. D. (1999). Lamellar bone: structure-function relations. *J. Struct. Biol.* **126**, 241-255.
- Wolfenson, H., Henis, Y. I., Geiger, B. and Bershadsky, A. D. (2009). The heel and toe of the cell's foot: a multifaceted approach for understanding the structure and dynamics of focal adhesions. *Cell Motil. Cytoskeleton* **66**, 1017-1029.
- Zamir, E., Katz, B. Z., Aota, S., Yamada, K. M., Geiger, B. and Kam, Z. (1999). Molecular diversity of cell-matrix adhesions. *J. Cell Sci.* **112**, 1655-1669.